Experiments in Fluids 2, 213–219 (1984)

Experiments in Fluids

Concentration and velocity measurements in the flow of droplet suspensions through a tube*

T. A. Kowalewski

Institute of Fundamental Technological Research, Polish Academy of Sciences, Swietokrzyska 21, 00-049 Warszawa, Poland

Abstract. Two optical methods, light absorption and LDA, are applied to measure the concentration and velocity profiles of droplet suspensions flowing through a tube. The droplet concentration is non-uniform and has two maxima, one near the tube wall and one on the tube axis. The measured velocity profiles are blunted, but a central plug-flow region is not observed. The concentration of droplets on the tube axis and the degree of velocity profile blunting depend on relative viscosity. These results can be qualitatively compared with the theory of Chan and Leal.

List of symbols

- a particle radius, m
- $\bar{a}$ $= a/R$, non-dimensional particle radius
- c volume concentration of droplets in suspension, m^3/m^3
- c_s stream-average volume concentration of droplets in suspension, m^3/m^3 $= \left(2\pi \int_0^R c\, v\, r\, dr\right) \Big/ \left(2\pi \int_0^R v\, r\, dr\right)$
- D $= 2R$, tube diameter, m
- L optical path length, m
- L_{ij} path length of laser beam through the j-th concentric layer when the beam crosses the tube diameter at the point on the inner circumference of the i-th layer, m
- N exponent in Eqs. (3) and (4)
- Q volumetric flowrate of suspension, m^3/s, $= 2\pi \int_0^R v\, r\, dr$
- R tube radius, m
- Re $= \varrho_s v_s D/\mu_c$, flow Reynolds number
- r radial position ($r = 0$ on a tube axis), m
- $\bar{r}$ $= r/R$, non-dimensional radial position
- v velocity of suspension, m/s
- $\bar{v}$ $= v/v_s$, non-dimensional velocity
- v_0 centre-line velocity of suspension ($r = 0$), m/s
- v_s $= Q/\pi R^2$, stream-average velocity of suspension, m/s
- x streamwise position ($x = 0$ at tube inlet), m
- $\bar{x}$ $= x/D$, non-dimensional streamwise position
- ϱ_c density of continuous phase, kg/m^3
- ϱ_d density of dispersed phase, kg/m^3
- ϱ_s stream-average density of suspension, kg/m^3, equals density when homogenized
- $\Delta\varrho$ $= \varrho_d - \varrho_c$, phase density difference, kg/m^3
- μ_c viscosity of continuous phase, Pa · s
- μ_d viscosity of dispersed (droplet) phase, Pa · s
- λ $= \mu_d/\mu_c$, viscosity ratio
- γ interfacial tension, N/m

* This work was financially supported by the National Science Foundation (USA) through an agreement no. J-F7F019P, M. Sklodowska-Curie fund

1 Introduction

Two phase flow started to gain attention from the moment when Segré and Silberberg (1962) studying the flow of dilute solid particle suspension through a tube, found that the particles tend to concentrate midway between the tube wall and its axis. Later, Karnis et al. (1966) showed that such particle migration is complex and depends on both flow conditions and particle size.

From the point of view of applications, the case of dense suspensions is most interesting. However, when the stream-average concentration of particles is greater than 1% the interparticle interactions cannot be neglected, and so the problem becomes difficult, both experimentally and theoretically. Two basic flow characteristics are important: the particle concentration profile and the velocity profile. The first measurements of both profiles were made by Karnis et al. (1966) by direct observation of single tracer particles added to a suspension. However, due to the tedious technique, the results obtained were meagre.

The main aim of the present work was to develop more accurate and convenient techniques for studying flows of highly concentrated suspension. For the measurement of the particle concentration a laser optical method was developed, and for measurement of velocity, the well known Laser Doppler Anemometry (LDA) technique was adapted. It was found possible to apply these optical methods to dense suspensions when the phases were closely matched in refractive index, so the suspension was optically homogeneous. In this paper we describe details of the experimental techniques and report some results obtained for the flow of droplet suspensions.

2 Experimental

Particle concentration and suspension velocity were measured separately in two different experiments on the same flow system. The droplet suspensions were prepared in the same way and had similar properties, except that for concentration measurements the dispersed phase (droplets) was dyed to obtain sufficient light absorption.

2.1 The flow system

A constant stroke pump provided steady flow through a 17.8 mm i.d., 150 cm long, vertically mounted glass tube, Fig. 1. Square cells with windows, filled with the immersion liquid, were fitted around the tube at four different points along the tube. At the tube ends mixing cells helped to achieve a uniform particle distribution at the flow inlet. To obtain the velocity measurements, the flow tube could be moved perpendicularly to the optical axis of the fixed anemometer by means of a micrometer screw. The position of the measuring volume within the tube was determined with an accuracy of 0.05 mm.

The flow rate could be changed both electrically by means of the motor voltage control and mechanically by a gear system in the range $0.1-100\ cm^3/s$. However, because of excessively high pressures developed at flow rates above $15\ cm^3/s$, some measurements were limited to this value of flow rate. The flow rate was estimated by measuring the angular speed of the driving shaft of the pump. The flow direction could be changed with valves. Droplet suspensions were prepared by pumping the liquid to be suspended through a hypodermic needle into a vessel containing the liquid of the continuous phase. The suspension was then passed through a device producing constant shear flow between two coaxial cylinders, one rotating at constant speed inside the other. Here the final maximum droplet size was adjusted, determined by the shear rate in the gap between cylinders. The distribution of droplets size in suspension entering and leaving the flow tube was analyzed under a microscope with the help of a photo camera and compared with observations of droplets size in the supplying tank. It was found that during the experiment the mean droplet size in suspension was constant within few percent error with the standard deviation in diameter of about ± 50%.

2.2 Materials

The glass tube was of no. 732-01 Pyrex by Sovirel, the refractive index $n_D = 1.474$. The two liquids for a suspension were prepared so, that they had the same refractive index for the laser light within $\pm 10^{-5}$ units. This matching was not possible solely by refractometry, and the final adjustment was achieved by tedious trials in which the laser beam was sent through the tested suspension upon a target for visual observation. The small differences between refractive indices of suspension and the glass (0.005) have no significant influence on the accuracy of measurements taken at distances greater than 0.2 mm from the tube wall.

The interfacial tension was measured with the method described by Mason and Clark (1965).

The range of the stream-average concentration of suspended droplets was $c_s = 0.05 - 0.4$. The relative mean droplet size was $\bar{a} = 0.01 - 0.06$. To cover a wide range of the viscosity ratio λ of dispersed to continuous phase, the measurements of droplet concentration profiles were performed for four different systems of suspensions labelled A, B, C, D, and the velocity profile measurements were done for three different systems labelled E, F, G. The properties of these systems are shown in Table 1.

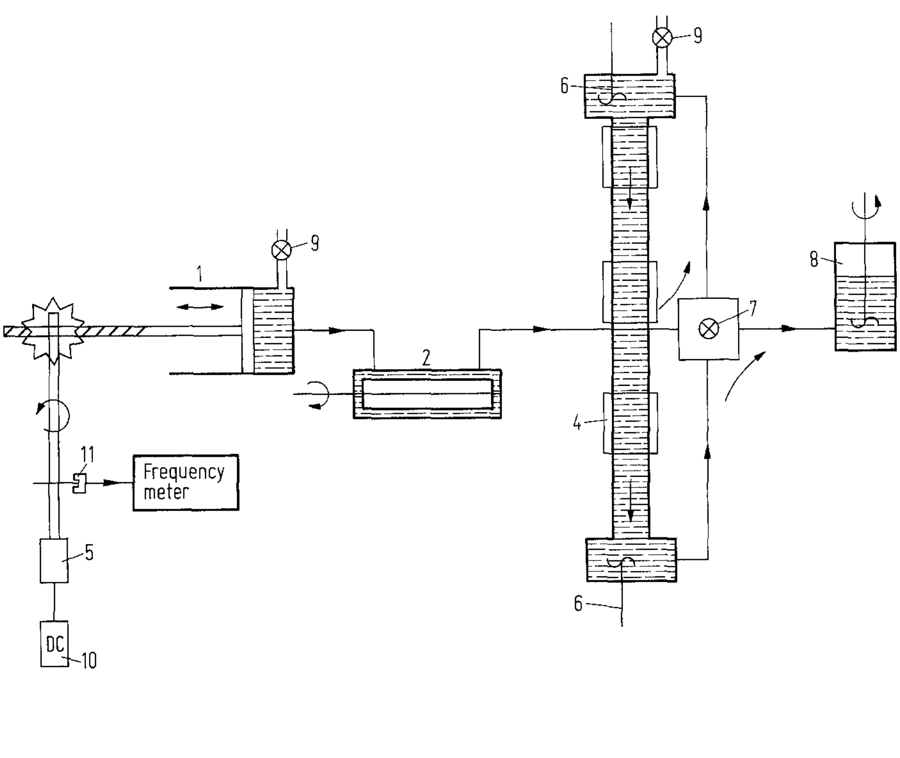

Fig. 1. The flow system: *1* pump; *2* Couette mixer; *3* flow tube; *4* cell with immersion liquid; *5* motor; *6* stirrer; *7* valves; *8* tank with breaker; *9* air valves; *10* reg. d.c. power supply; *11* revolution meter

Table 1. Description of systems and physical properties of fluids, 295 °K

System	Continuous phase	Dispersed phase	μ_c, Pa·s	λ	$\Delta\varrho$, kg/m³	γ, *N/m*	*Re*
A	glycerine + water + ammonium iodide	tetrachlorethane + silicon oil + dye [a]	0.053	0.07	$1 \cdot 10^{-6}$	0.016	0.3 –50
B	paraffin oil	castor oil + methanol + methyl phthalate + dye [b]	0.190	0.15	$2 \cdot 10^{-4}$	0.005	0.06–30
C	paraffin oil	castor oil + methyl phthalate+dye [b]	0.190	1.7	$1.6 \cdot 10^{-4}$	0.008	0.06–30
D	glycerine + ammonium iodide	castor oil + dye [c]	0.091	7.2	$4 \cdot 10^{-4}$	0.017	0.12–60
E	castor oil	glycerine + ammonium iodide + water	0.9	0.09	$3.9 \cdot 10^{-4}$	–	0.05–1.8
F	castor oil + methyl phthalate	paraffin oil	0.35	0.58	$8 \cdot 10^{-5}$	–	0.12–4.6
G	castor oil + methyl phthalate + methanol	paraffin oil	0.049	4.2	$7 \cdot 10^{-5}$	–	0.9 –30

[a] Ferro Enamds Blue Dye PC42 – Holland; [b] Methylviolett 2B, Loba-Chemie – Austria; [c] Oil Green G, Zachem-Poland

2.3 Particle distribution measurements

2.3.1 Method

The present measurements are based on the principle of light absorption by dyed suspended droplets. To obtain concentrations, use is made of the Lambert-Beer law:

$$I = I_0 \exp(-k\,c\,L), \tag{1}$$

where I_0 and I are the light intensities before and after passing through the sample, k is the extinction coefficient, and L is the length of the light path across the sample.

The flow tube is scanned laterally by a laser beam which describes parallel chords across the circular tube cross-section. In the numerical data treatment the flow axial symmetry is assumed, and the tube cross section is divided into n concentric layers of equal thickness. In order to simplify calculations we take into account only a quadrant of the tube cross-section, Fig. 2. The layers are labelled $1, 2, \ldots, n$ from the outside rim. Laser beam positions are labelled likewise. The length of the i-th light path through the j-th flow layer is L_{ij} and can be easily calculated from the Pitagorean theorem. The concentration distribution is determined by solving the set of n algebraic equations:

$$I_i = I_0 \exp\left(-k \sum_{j=1}^{n} c_j L_{ij}\right), \tag{2}$$

$i = 1, 2, \ldots, n$, I_i is the intensity of the emergent laser beam along the i-th chord, and c_j is the droplet concentration in the j-th layer.

The chosen value of n was 100.

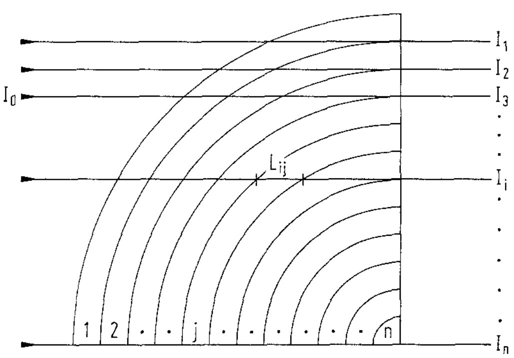

Fig. 2. The scheme of concentration calculations

2.3.2 Apparatus

The optical system which forms a 50 µm dia. laser beam for scanning the tube cross-section is shown in Fig. 3. The beam from a He-Ne laser source is first collimated by diaphragms and focused by a 105 mm lens on a 10 µm pinhole aperture. The beam is then collected by a 30 mm lens and reflected by a mirror which rotates at constant speed (usually 15 r.p.s.). The axis of revolution is normal to the incident beam and located at the focus of a third lens. Hence, for each position of the mirror the light beam emerging from this lens is parallel to the lens axis, changing position only in the direction normal to the axis. The electric signal from the receiving photodiode was registered digitally by a special signal analyzer (ANOPS 100, produced at Warsaw Polytechnic) allowing automatic averaging of the required set of measurements in memory (usually from 5 to 8 single mirror revolutions). The absorption curves obtained in this way, before the final computation described above, were smoothed numerically by the least squares method. The device allows measurements of the local concentration with spatial resolution of about 100 µm. Reproducibility of the local concentration values was within 10% standard deviation error. The calculated stream-average concentration was constant within 2% standard deviation error.

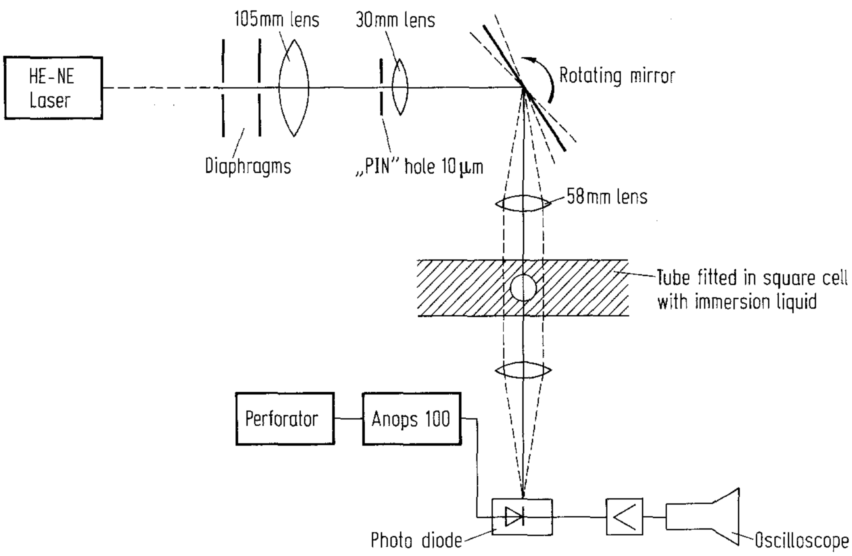

Fig. 3. The optical system for concentration measurements

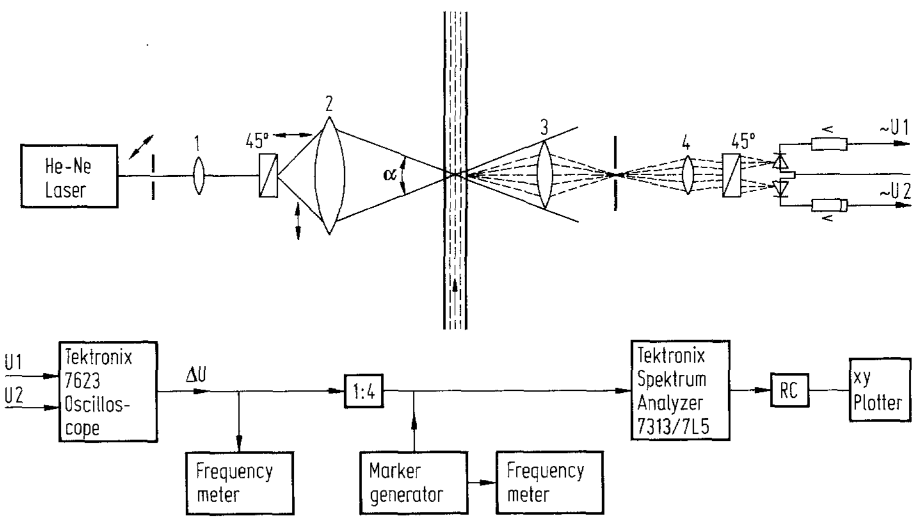

Fig. 4. The Laser-Doppler system

2.4 Velocity profile measurements

A differential Doppler system (Fig. 4) with optical compensation for removing the pedestal was employed. This technique, developed by Bossel et al. (1979), uses laser beams polarized at right angles by a Wollaston prism. The scattered light is analyzed by a second Wollaston prism and received by two detectors. The signals are 180° out of phase, so by subtracting them the background light arriving in phase at the detectors is removed. To obtain a Doppler frequency, the signal from the detectors was sent through the differential input of a Tektronix 7623 oscilloscope and, together with a marker signal from an external generator, into a Tektronix Spectrum Analyzer 7313/7L5. The spectrum was analyzed within 100 s full-scale span time, observed on the screen and recorded by XY plotter. Such an arrangement made it possible to measure very low frequencies of multiparticle Doppler signals (from about 30 Hz), considerably below the range of ordinary frequency trackers used for LDA. The accuracy of measured Doppler frequencies was about 0.5–2%, depending on the frequency. The velocity measurements were performed at a distance of 50 cm from the tube inlet, for 7 to 12 different points on the tube radius. The spatial resolution of the system was about 0.1 mm except for the region of about 0.2 mm from the tube wall where, due to the effect of the residual difference in refractive indices of the tube glass and the medium, measurements were impossible. As the two phases of the suspension had closely matched refractive indices, there was no laser light scattering by droplets. However, it was found that sufficient LDA signal could be obtained from light scattered by impurities present in the liquids – so no extra seeding was needed.

3 Results

3.1 Particle distribution

The main finding of the present measurements is the non-uniform concentration of droplets along the tube radius, with a characteristic double-humped shape, Fig. 5. It was observed that for suspensions of low relative viscosity λ (systems A and B), the value of the central maximum increases and that of the side maximum decreases as the distance from the tube inlet x grows. The reverse relation was observed for high relative viscosity (systems C and D) in which case the central maximum decreases with distance from the tube inlet.

It was also observed that the radial position of the side maximum for the tested systems shifts in a relatively narrow range (0.15–0.25 tube radii from the tube wall) towards the tube axis as the distance from the tube inlet or the flow Reynolds number grows (Figs. 6, 7).

The stream-average concentration of droplets in the tested range, $c_s = 0.05-0.4$, has relatively small influence on the concentration profiles, mainly smoothing the double-humped shape with a small shift of the side maximum closer to the tube wall for higher values of particle concentration.

3.2 Velocity profile

The present measurements show velocity profile blunting for the flow of all the tested suspensions. Because of the high accuracy of the LDA measurements, it was possible to determine that even near the tube axis there still are measurable velocity gradients and thus a plug flow region does not occur.

The blunted parabolic shape of the measured velocity profiles is well described by the formula proposed in previous ultrasonic measurements (Kowalewski 1980):

$$v = v_0 (1 - \bar{r}^N) . \tag{3}$$

The exponent N is an indicator of the profile blunting. In non-dimensional form eq. (3) reads

$$\bar{v} = \frac{N+2}{N} (1 - \bar{r}^N) . \tag{4}$$

The value of N was determined from this equation by least-squares fitting of the experimental data.

The dependence of the profile-blunting characteristic N on the stream-average concentration of droplets c_s is shown in Fig. 8. Measurements performed for suspensions of low relative viscosity λ (system E) are compared with some available data for the flow of similar suspensions.

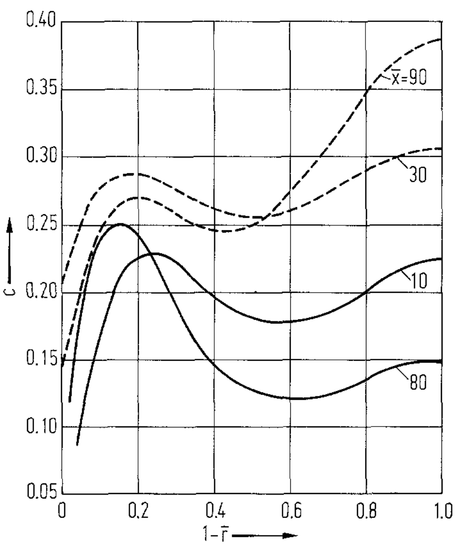

Fig. 5. Droplet concentration profiles:

Symbol	λ	$\bar{a}$	c_s	Re
......	0.07	0.05	0.28	12
——	7.2	0.02	0.2	30

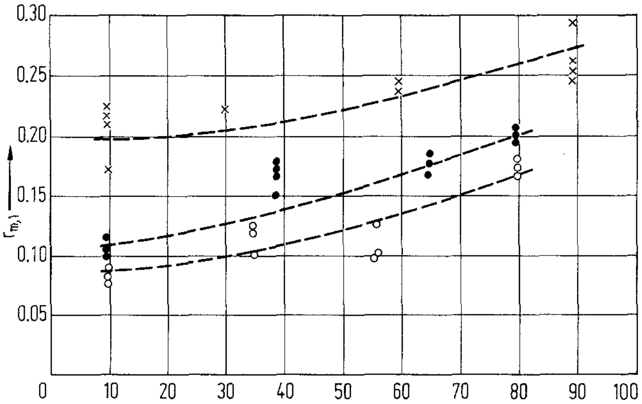

Fig. 6. The relative distance from the wall of the side maximum as a function of the distance from the tube inlet:

Symbol	λ	$\bar{a}$	c_s	Re
×	0.07	0.013	0.22	35
●	0.15	0.01	0.4	0.4
○	1.7	0.02	0.2	30

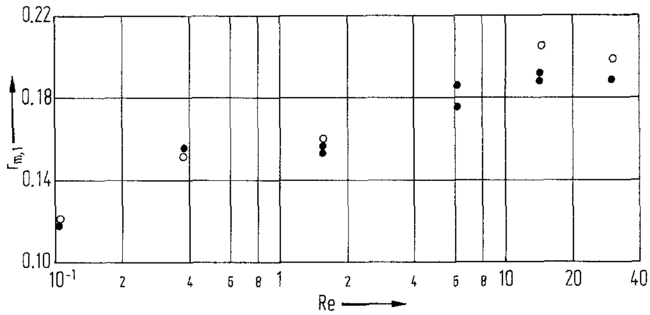

Fig. 7. The relative distance from the wall of the side maximum as a function of the Reynolds number: $\lambda = 0.15$, $\bar{a} = 0.01$, $c_s = 0.05$. Closed circles: $\bar{x} = 10$; open circles: $\bar{x} = 80$

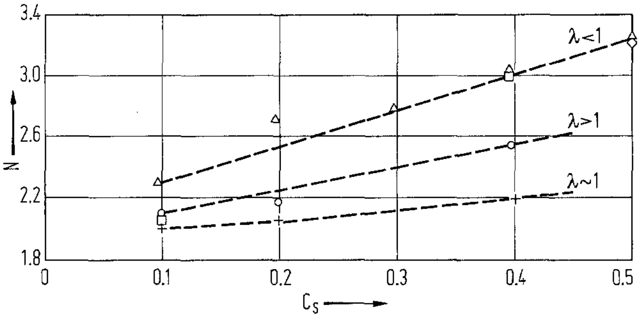

Fig. 8. Velocity profile blunting parameter vs. concentration of droplets:

Symbol	λ	$\bar{a}$	*Re*	References
○	4.2	0.01	0.9	LDA measurements
□	0.09	0.01	0.1	LDA measurements
+	0.58	0.01	0.12	LDA measurements
△	0.01	0.02	10	ultrasound measurements, Kowalewski (1980)
◇	0.16	0.02	0.02	visual measurements, Vadas et al. (1976)

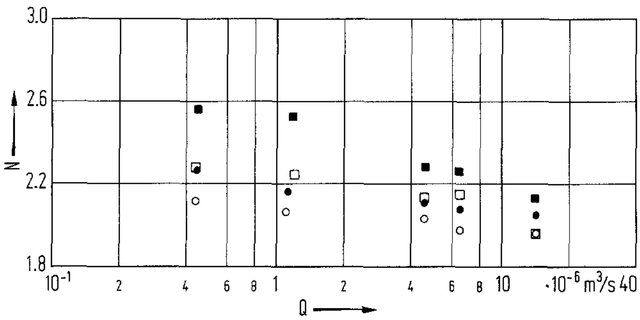

Fig. 9. Velocity profile blunting parameter vs. flow rate:

Symbol	λ	c_s
○	0.58	0.2
●	0.58	0.4
□	4.2	0.2
■	4.2	0.4

There are no reports on suspensions of highly viscous droplets to compare with our results for systems F and G.

As can be seen in Fig. 8, velocity profiles at low volume concentrations of droplets ($c_s = 0.1$) exhibit very slight blunting ($N \approx 2$). The blunting increases markedly at higher concentrations ($c_s = 0.4$). The value of the blunting parameter N depends also on the viscosity ratio λ and the flow rate Q. It is evident that the degree of blunting is minimal for suspensions with the smallest viscosity difference between the phases (indicated by system F). The effect of the flow rate is shown in Fig. 9. The degree of blunting generally decreases with increasing flow rate.

4 Discussion

The results provide insight into the flow of concentrated suspension of droplets. The observed effects, namely non-uniform droplet distribution and deviations from the parabolic velocity profile, are undoubtedly due to the hydrodynamic interactions of droplets with each other and with the tube wall. Unfortunately, a theoretical treatment of particle behaviour in tube flow of such dense suspensions is not yet available.

The problem of migration of a single deformable droplet in a unidirectional shearing flow, both with and without shear-rate gradients, has been theoretically considered by Chan and Leal (1979). They show that cross-flow migration of the droplet depends on the magnitude of its deformation which is proportional to the non-dimensional parameter $v_0 \cdot \mu_c / \gamma$, the size of the drop, and the viscosity ratio λ. Their analysis considers two distinct cases: droplet close to the wall, and droplet in unbounded flow (far from the walls). In the first case the predicted direction of droplet migration is for all λ towards the flow axis and its velocity decreases hyperbolically with distance from the wall. In the second case, in contradiction to previous theoretical and experimental reports, the direction of droplet migration depends on the viscosity ratio λ; for $\lambda < 0.5$ or $\lambda > 10$ the migration is predicted to occur in the direction of the flow axis, but for intermediate values, $0.5 < \lambda < 10$, migration is predicted to occur in the direction of the nearest wall. The velocity of this migration is proportional to the distance from the flow axis.

It is not possible to quantitatively compare this theory with the presented experiments conducted for highly concentrated suspensions. There are, however, some qualitative indications that help to explain the present observations. The existence of a concentration maximum near the tube wall, observed for all tested suspensions, may be understood as a consequence of short-range interaction between droplets and the tube wall. Droplets develop this maximum when forced away from the wall. At a short distance from the tube wall this force becomes negligible and due to the interaction with the "unbounded" velocity field the droplets slowly migrate from the wall. This migration occurs in the direction to the flow axis for viscosity ratios $\lambda < 0.5$ or $\lambda > 10$, but for intermediate values also from the flow axis to a point where the lateral force induced by the flow field is equal in value to the force induced by the wall.

The present observations show that the concentration of droplets at the tube axis depends on the relative viscosity λ, as is predicted by the Chan and Leal theory; for small λ (systems A and B) the peak of concentration on the axis grows with distance from the inlet; for high λ (systems C and D) this peak decreases with the distance from the inlet. It can be expected that at a large distance from the inlet both observed concentration peaks will meet at an equilibrium position, on the flow axis or between the tube wall and the flow axis. The present observations confirm this trend, however, the asymptotic behaviour of concentration profiles was not investigated. This was due to the fact that for much longer flow tubes droplet coalescence could not be neglected. The Chan and Leal theory does not allow for predicting such an equilibrium position for our highly concentrated suspensions.

The distribution of droplets across the tube may influence the velocity profile of a suspension by changing the local effective viscosity, but there is no apparent correlation between concentration and velocity profiles. The observed velocity profile blunting depends mainly on the stream-average concentration and on the relative viscosity λ. The lowest value of blunting is observed for the system of almost equal viscosities of the phases (system F). This is perhaps due to smaller damping of the velocity gradients when the viscosity of the droplet liquid is close to that of the carrier medium.

The flow-rate dependence of the velocity profile blunting points to non-Newtonian behaviour of the droplet suspension, but available rheological models do not seem adequate to explain the observed effects. The velocity profile described by eq. (4) suggests a power-law model of a pseudoplastic liquid, but the observed values of the velocity profile blunting parameters N are much higher than those indicated by viscosity measurements with a shear viscosimeter for the same suspension (Goldsmith and Marlow 1979). Thus it seems that non-uniform concentration of droplets in the tube and the effects of screening of the velocity gradients by neighbouring droplets are not included in rheological description of suspensions.

Acknowledgements

I thank Professor W. Fiszdon and Dr. R. Herczyński of the Polish Academy of Sciences for their guidance and critical remarks concerning present experiments. I also owe special thanks to Professor E. A. Müller and Dr. G. E. A. Meier of the Max-Planck Institut in Göttingen whose hospitality and help made the LDA measurements possible.

References

Bossel, H. H.; Hiller, W. J.; Meier, G. E. A. 1972: Noise cancelling signal difference method for optical velocity measurements. J. Phys. E 5, 893–896

Chan, P. C.-H.; Leal, L. G. 1979: The motion of deformable drop in a second-order fluid. J. Fluid Mech. 92, 131–170

Goldsmith, H. L.; Marlow, J. C. 1979: Flow behaviour of erythrocytes. J. Colloid Interface Sci. 71, 383–407

Karnis, A.; Goldsmith, H. L.; Mason, S. G. 1966: The flow of suspensions through tubes. Can. J. Chem. Eng. 44, 181–193

Kowalewski, T. A. 1980: Velocity profiles of suspension flowing through a tube. Arch. Mech. 32, 857–865

Mason, G.; Clark, W. C. 1965: Liquid bridges between spheres. Chem. Eng. Sci. 20, 861–862

Segré, G.; Silberberg, A. 1962: Behaviour of macroscopic rigid spheres in Poisseuille flow. J. Fluid Mech. 14, 136–157

Vadas, E. B.; Goldsmith, H. L.; Mason, S. G. 1976: The microrheology of colloidal dispersions. Trans. Soc. Rheol. 20, 373–407

Received December 27, 1983